

An outlier-robust Kalman filter with mixture correntropy

Hongwei Wang^a, Wei Zhang^a, Junyi Zuo^a, Heping Wang^a

^a*School of Aeronautics, Northwestern Polytechnical University, Xi'an, People's Republic of China, 710072*

Abstract

We consider the robust filtering problem for a nonlinear state-space model with outliers in measurements. A novel robust cubature Kalman filtering algorithm is proposed based on mixture correntropy with two Gaussian kernels. We have formulated the robust filtering problem by employing the mixture correntropy induced cost to replace the quadratic one in the conventional Gaussian approximation filter for the measurement fitting error. In addition, a tradeoff weighting coefficient is introduced to make sure the proposed approach can provide reasonable state estimates in scenarios with small measurement fitting errors. The robust filtering problem is iteratively solved by using the cubature Kalman filtering framework with a reweighted measurement covariance. Numerical results show that the proposed method can achieve a performance improvement over existing robust solutions.

Keywords: Robust Kalman filter, mixture correntropy, cubature Kalman filter, state estimation

1. Introduction

State estimation for stochastic discrete-time dynamic systems is one of the vital issues in control engineering, and it has broad applications in various areas, such as target tracking, sparse signal processing, fault detection and diagnosis, information fusion, and many others [1–5]. The state estimates of a linear system with Gaussian noises is provided by the celebrated Kalman filter [6]. For nonlinear systems with a Gaussian assumption (i.e., both the process and measurement noises are Gaussian), several Kalman-like Gaussian approximation filters (GKF) were investigated, e.g., the unscented Kalman filter [7], cubature Kalman filter [8, 9], to name a few. These solutions have shown good performance when the Gaussian assumption meets in systems. In some applications, however, the Gaussian assumption for the measurement noise may fail since outliers may contaminate measurements due to unreliable sensors. Outliers lead to the measurement noise having a heavy tail and becoming non-Gaussian, resulting in a substantial degradation of the existing GKF.

The sequential Monte-Carlo sampling/particle filter (PF) [10] and the Gaussian sum filter (GSM) are two general strategies to deal with non-Gaussian noises caused by measurement outliers. In the PF, a massive number of particles are involved to approximate the posterior probability density function to obtain a reasonable estimation results. In the GSM, the state estimates are obtained by combining the results from several parallelly implemented filters via an interacting procedure. Therefore, both the PF and GSM suffer from a great computational burden, which prevents them from being widely used in applications. In addition, a computationally economical approach, i.e., integrating the robust cost from M -estimation (e.g., Huber's cost) into the GKF framework [11–13], has also been studied. This type of robust filters were developed by interpreting the GKF filtering problem as a linear or nonlinear regression. Other approaches for robust filtering such as the heavy-tailed distribution based solution [14] and the H_∞ filter [15] were also reported in literatures.

Recently, a novel local similarity measure called correntropy from information theoretic learning is introduced to deal with heavy-tailed non-Gaussian noises [16–18], and its associated maximum correntropy criterion (MCC) has been employed to design a robust filtering algorithm. In [19, 20] the MCC was first employed to improve the robustness of the KF for linear systems. Those methods employed the gradient descent approach and ignored the covariance propagation procedure, which may cause a potential loss of information. To handle this issue, a robust Kalman filter called MCKF [21] was developed via recasting the Kalman filtering problem as a linear regression. Afterward, several variants of the MCKF were developed for nonlinear systems [22–24]. Although the feasibility of the MCC based robust filters for dealing with non-Gaussian noises has been demonstrated, the default kernel in the

MCC, e.g., the Gaussian kernel, may not sufficient to deal with more complexity data in many practical problems [25]. Besides, there is still no guideline for selection of the kernel parameter which has a significant influence of the MCC associated robust filter.

In this paper, we propose a new robust Kalman filter based on mixture correntropy. We formulate the robust filtering problem by utilizing a mixture correntropy induced loss to replace the quadratic one in the GKF for measurement fitting errors. In addition, a weighting coefficient is included to seek a tradeoff between model and measurement fitting errors. The resulting robust filtering problem is finally iteratively solved within the GKF framework with a reweighted measurement covariance. The simulation results have shown the superior performance of the proposed algorithm, and also provide a heuristic rule to design kernel parameters.

The remaining of the paper is organized as follows. In Section 2, we give a brief introduction of mixture correntropy. In section 3, we formulate the mixture correntropy based robust Kalman filtering problem, and derive a robust filter. In Section 4 we present a simulation example to verify the performance of the proposed algorithm. Finally Section 5 concludes our work.

2. Brief Review of Mixture Correntropy

For two random variables X and Y , correntropy, a similarity measure from information theoretic learning, is defined by [16]

$$V(X - Y) = E[\kappa(X - Y)] = \int \int \kappa(X - Y)p(x, y)dxdy \quad (1)$$

where $\kappa(\cdot, \cdot)$ is a kernel function which satisfies Mercer's theorem, $E(\cdot)$ denotes the expectation operation and $p(x, y)$ is the joint probability density function of X and Y . In practice, the data samples $\{x_i, y_i\}_{i=1}^N$ are generally available rather than $p(x, y)$, hence the correntropy can be approximated by (2) when utilizing the frequently used Gaussian kernel,

$$V(X, Y) \approx \frac{1}{N} \sum_{i=1}^N \exp\left(-\frac{e_i^2}{2\sigma^2}\right) \quad (2)$$

where $e_i = x_i - y_i$ and σ is the parameter of the Gaussian kernel. Although the Gaussian kernel is a default in correntropy owing to its excellent performance, it may not sufficient to deal with more complex data. To address this and improve the flexibility, a mixture correntropy is introduced, i.e.,

$$M(X, Y) = E[\alpha\kappa_1(X, Y) + (1 - \alpha)\kappa_2(X, Y)] \quad (3)$$

where $\kappa_1(\cdot, \cdot)$ and $\kappa_2(\cdot, \cdot)$ are two different Mercer kernel functions and $\alpha \in [0, 1]$ is a mixture coefficient. Here the difference between $\kappa_1(\cdot, \cdot)$ and $\kappa_2(\cdot, \cdot)$ are twofold. On the one hand, $\kappa_1(\cdot, \cdot)$ and $\kappa_2(\cdot, \cdot)$ can be the kernels sharing the same structure but with different parameters, e.g., the one studied in this work (see below). On the other, $\kappa_1(\cdot, \cdot)$ and $\kappa_2(\cdot, \cdot)$ may be the different types of kernel functions, e.g., a combination of the Gaussian kernel and Laplace kernel in [25]. In addition, the mixture correntropy can also be extended to a more general one with more than two different kernel functions. For the sake of simplicity, in this paper, we consider a mixture correntropy with two Gaussian kernels with the different parameters, which can be approximated by

$$M(X, Y) = \frac{1}{N} \sum_{i=1}^N \left(\alpha \exp\left(-\frac{e_i^2}{2\sigma_1^2}\right) + (1 - \alpha) \exp\left(-\frac{e_i^2}{2\sigma_2^2}\right) \right) \quad (4)$$

When $\alpha = 0$ or $\alpha = 1$, the mixture correntropy degrades the conventional correntropy. With a proper α , the mixture correntropy can achieve a better performance than the conventional one, see details in Section 4.

Clearly, the mixture correntropy $M(X, Y)$ meets its maximum 1 when $X = Y$. Therefore akin to the C-loss associated to the conventional correntropy, we here define the mixture C-loss as

$$L(X, Y) = 1 - M(X, Y) \quad (5)$$

With N data samples $\{x_i, y_i\}_{i=1}^N$ and two Gaussian kernels, the empirical mixture loss, called double-Gaussian mixture correntropy loss (DG-MCL), is calculated by

$$L(X, Y) = 1 - \frac{1}{N} \sum_{i=1}^N \left(\alpha \exp\left(-\frac{e_i^2}{2\sigma_1^2}\right) + (1 - \alpha) \exp\left(-\frac{e_i^2}{2\sigma_2^2}\right) \right) \quad (6)$$

3. Derivation of the proposed robust Kalman filter

3.1. Cost Function

Consider the stochastic dynamic process described by a state space model

$$\mathbf{x}_t = f(\mathbf{x}_{t-1}) + \mathbf{w}_{t-1} \quad (7)$$

$$\mathbf{y}_t = h(\mathbf{x}_t) + \mathbf{v}_t \quad (8)$$

where $\mathbf{y}_t \in \mathcal{R}^m$ is a measurement related the state of interest $\mathbf{x}_t \in \mathcal{R}^n$; $f(\cdot)$ and $h(\cdot)$ are some known mappings to model the state evolution and measurement procedure respectively; $\mathbf{w}_{t-1} \sim \mathcal{N}(0, \mathbf{Q}_{t-1})$ is the process noise and \mathbf{v}_t is the measurement noise. In canonical Kalman filtering, \mathbf{v}_t is assumed to be Gaussian, i.e., $\mathbf{v}_t \sim \mathcal{N}(0, \mathbf{R}_t)$. Under such a Gaussian assumption, the Kalman filtering problem is formulated as

$$\hat{\mathbf{x}}_{t|t} = \arg \min_{\mathbf{x}_t} \left(\frac{1}{2} \|\mathbf{x}_t - \hat{\mathbf{x}}_{t|t-1}\|_{\mathbf{P}_{t|t-1}}^2 + \frac{1}{2} \|\mathbf{y}_t - h(\mathbf{x}_t)\|_{\mathbf{R}_t}^2 \right) \quad (9)$$

where $\hat{\mathbf{x}}_{t|t-1}$ and $\mathbf{P}_{t|t-1}$ are the predicted state and associated error covariance (see details in Appendix A).

In order to deal with outliers in measurements, we utilize the DG-MCL to replace the quadratic loss for the measurement fitting error, resulting the following robust filtering problem

$$\hat{\mathbf{x}}_{t|t} = \arg \min_{\mathbf{x}_t} \left\{ \frac{1}{2} \|\mathbf{x}_t - \hat{\mathbf{x}}_{t|t-1}\|_{\mathbf{P}_{t|t-1}}^2 + \lambda \left[1 - \frac{1}{m} \sum_{i=1}^m \left(\alpha \exp\left(-\frac{e_{t,i}^2}{2\sigma_1^2}\right) + (1 - \alpha) \exp\left(-\frac{e_{t,i}^2}{2\sigma_2^2}\right) \right) \right] \right\} \quad (10)$$

where $e_{t,i}$ is the i th component of $\mathbf{e}_t = \mathbf{R}_t^{-1/2}(\mathbf{y}_t - h(\mathbf{x}_t))$ and λ is a weighting coefficient to make the balance between the model fitting error and measurement fitting error. λ should be carefully chosen to obtain a reasonable estimation result. Specifically, we expect that the performance of the DG-MCL is similar as that of the quadratic loss when the measurement fitting error is small. We note that for a small real vale δ , $e^\delta \approx 1 + \delta$. Hence for some small $e_{t,i}$, the DG-MCL can be approximated as

$$L \approx \frac{\alpha\sigma_2^2 + (1 - \alpha)\sigma_1^2}{m\sigma_1^2\sigma_2^2} \frac{1}{2} \sum_{i=1}^m e_{t,i}^2 \quad (11)$$

Clearly, λ can be determined as

$$\lambda = \frac{m\sigma_1^2\sigma_2^2}{\alpha\sigma_2^2 + (1 - \alpha)\sigma_1^2} \quad (12)$$

3.2. Derivation

In this section, we derive the robust Kalman filter. For simplicity, we denote the Gaussian kernels in (10) by $G_1(e)$ and $G_2(e)$ respectively, and thus the DG-MCL related robust Kalman filtering is rewritten as

$$\hat{\mathbf{x}}_{t|t} = \arg \min_{\mathbf{x}_t} \left\{ \frac{1}{2} \|\mathbf{x}_t - \hat{\mathbf{x}}_{t|t-1}\|_{\mathbf{P}_{t|t-1}}^2 + \lambda \left(1 - \frac{1}{m} \sum_{i=1}^m \alpha G_1(e_i) + (1 - \alpha) G_2(e_i) \right) \right\} \quad (13)$$

Differencing the cost function in (13) with regards to \mathbf{x}_t we have

$$\mathbf{P}_{t|t-1}^{-1}(\mathbf{x}_t - \hat{\mathbf{x}}_{t|t-1}) - \frac{\lambda}{m} \sum_{i=1}^m \left(\alpha \frac{\partial G_1(e_i)}{\partial e_i} \frac{\partial e_i}{\partial \mathbf{x}_t} + (1-\alpha) \frac{\partial G_2(e_i)}{\partial e_i} \frac{\partial e_i}{\partial \mathbf{x}_t} \right) = 0 \quad (14)$$

We know that

$$\frac{\partial G_1(e_i)}{\partial e_i} = -\frac{e_i}{\sigma_1^2} G_1(e_i), \quad \frac{\partial G_2(e_i)}{\partial e_i} = -\frac{e_i}{\sigma_2^2} G_2(e_i) \quad (15)$$

Substituting (15) into (14) results in

$$\mathbf{P}_{t|t-1}^{-1}(\mathbf{x}_t - \hat{\mathbf{x}}_{t|t-1}) + \frac{\lambda}{m} \sum_{i=1}^m \left(\frac{\alpha G_1(e_i)}{\sigma_1^2} + \frac{(1-\alpha) G_2(e_i)}{\sigma_2^2} \right) \frac{e_i \partial e_i}{\partial \mathbf{x}_t} \quad (16)$$

Define a diagonal matrix $\mathbf{\Lambda}_t$ with its i th entry given by

$$\Lambda_{t,ii} = \frac{\lambda}{m} \left(\frac{\alpha G_1(e_i)}{\sigma_1^2} + \frac{(1-\alpha) G_2(e_i)}{\sigma_2^2} \right) \quad (17)$$

and then (16) can be rewritten into the matrix format as

$$\mathbf{P}_{t|t-1}^{-1}(\mathbf{x}_t - \hat{\mathbf{x}}_{t|t-1}) + \frac{\partial \mathbf{e}_t}{\partial \mathbf{x}_t} \mathbf{\Lambda}_t \mathbf{e}_t = 0 \quad (18)$$

Practically (18) is the derivative of the cost function of the following optimization problem

$$\hat{\mathbf{x}}_{t|t} = \arg \min_{\mathbf{x}_t} \left(\frac{1}{2} \|\mathbf{x}_t - \hat{\mathbf{x}}_{t|t-1}\|_{\mathbf{P}_{t|t-1}^{-1}}^2 + \frac{1}{2} \|\mathbf{y}_t - h(\mathbf{x}_t)\|_{\bar{\mathbf{R}}_t^{-1}}^2 \right) \quad (19)$$

where

$$\bar{\mathbf{R}}_t = \mathbf{R}_t^{T/2} \mathbf{\Lambda}_t^{-1} \mathbf{R}_t^{1/2} \quad (20)$$

Despite simple structure, directly solving (19) is intractable due to the fact the $\bar{\mathbf{R}}_t$ is dependent on the state \mathbf{x}_t via $\mathbf{\Lambda}_t$. To address this, we adopt an alternate iterative algorithm. Specifically, for the given estimate $\hat{\mathbf{x}}_{t|t}^k$ after the k th iteration, we construct $\mathbf{\Lambda}_t^k$ via (17), and then $\bar{\mathbf{R}}_t^k$ via (20). In the next iteration, we solve the optimization problem (19) with $\bar{\mathbf{R}}_t^k$ to obtain $\hat{\mathbf{x}}_{t|t}^{k+1}$. It is noted that (19) has a similar structure as the one under the Gaussian assumption illustrated in (9), which enables us to solve (19) by applying the existing Gaussian approximation filtering solutions, e.g., the CKF in Appendix A. This iteration loop continues until the algorithm converges, e.g., for small tolerance ϵ ,

$$\|\hat{\mathbf{x}}_{t|t}^{k+1} - \hat{\mathbf{x}}_{t|t}^k\| < \epsilon \quad (21)$$

At the beginning, we initial $\mathbf{\Lambda}_t$ as an identity matrix, meaning that in the first loop a conventional CKF is implemented. The proposed robust filter is summarized in Algorithm 1.

4. Simulations and Results

In this section, we analysis the proposed algorithm by investigating the state estimation for a Van der Pol oscillator (VPO). For comparison, we also consider the conventional CKF and some existing robust filters, including the maximum correntropy derivative-free robust CKF (MCC-CKF) [24], linear regression and maximum correntropy based CKF (RMCC-CKF) [22] and Huber's cost function based CKF (Huber-CKF) [13]. We use two different set in the MCC-CKF, i.e., the MCC-CKF1 with $\{\sigma = 100, \eta = 4\}$ and MCC-CKF2 with $\{\sigma = 100, \eta = 5\}$ (setting $\sigma = 100$ is to deal with the Gaussian process noise). We set the kernel parameter in the RMCC-CKF to 5 and the threshold

Algorithm 1 Robust CKF with Mixture Correntropy

Input: $y_{1:T}$, $\hat{\mathbf{x}}_{0|0}$, $\mathbf{P}_{0|0}$, $\mathbf{Q}_{1:T}$, $\mathbf{R}_{1:T}$, σ_1, σ_2 .
Output: $\hat{\mathbf{x}}_{t|t}$ and $\mathbf{P}_{t|t}$ for $t = 1 : T$.
for $t = 1 : T$ **do**
 Update $\{\hat{\mathbf{x}}_{t|t-1}, \mathbf{P}_{t|t-1}\}$ via $\{(A.4), (A.5)\}$;
 Initialize $k = 0$, $\mathbf{\Lambda}_t = \mathbf{I}_m$;
 repeat $k = 1, \dots$,
 Update $\bar{\mathbf{R}}_t$ via (20) using $\mathbf{\Lambda}_t$;
 Update $\hat{\mathbf{x}}_{t|t}^k$ and $\mathbf{P}_{t|t}^k$ via (A.11) and (A.12) respectively;
 Calculate $\mathbf{e}_t = \mathbf{R}_t^{-1/2}(\mathbf{y}_t - h(\hat{\mathbf{x}}_{t|t}^k))$, and update $\mathbf{\Lambda}_t$ via (17);
 Calculate $\epsilon = \|\hat{\mathbf{x}}_{t|t}^{k+1} - \hat{\mathbf{x}}_{t|t}^k\|$;
 until $\epsilon < 10^{-6}$
 $\hat{\mathbf{x}}_{t|t} = \hat{\mathbf{x}}_{t|t}^k$, $\mathbf{P}_{t|t} = \mathbf{P}_{t|t}^k$.
end for

parameter in the Huber-CKF to 1.345. In our DG-MCL-CKF, two kernel parameters are determined as $\sigma_1 = 4$ and $\sigma_2 = 5$ respectively, and the mixture coefficient α is 0.5.

The standard VPO model is given by

$$\begin{cases} \dot{x}_1 = x_2 \\ \dot{x}_2 = \mu(1 - x_1^2)x_2 - x_1 \end{cases} \quad (22)$$

where μ is a coefficient to control the nonlinearity of the VPO. Using the sampling interval δ to discretize the VPO results

$$\mathbf{x}_t = \mathbf{x}_{t-1} + \begin{pmatrix} \int_{t-1}^{t-1+\delta} x_2 dt \\ \int_{t-1}^{t-1+\delta} (\mu(1 - x_1^2)x_2 - x_1) dt \end{pmatrix} + \mathbf{w}_{t-1} \quad (23)$$

where $\mathbf{x}_t = [x_{1,t}, x_{2,t}]^T$ is the state of interest and \mathbf{w}_t is the process noise which is assumed to be Gaussian, i.e., $\mathbf{w}_t \sim \mathcal{N}(0, \mathbf{Q}_{t-1})$. We utilize the fourth-order Runge-Kutta scheme to numerically calculate the integral terms in (23) which in general have no analytical solutions. Furthermore we assume that the noisy measurements are gathered via

$$y_t = (x_{1,t} - 1)^2 + 1 + v_t \quad (24)$$

The measurement noise is modeled as the following Gaussian-mixture model to simulate the heavy-tailed property caused by outliers

$$v_t \sim (1 - \phi)\mathcal{N}(0, R_t) + \phi\mathcal{N}(0, \varphi R_t) \quad (25)$$

in which ϕ is the contaminating ratio, φ is the outlier strength factor and R_t is the covariance of the nominal measurement noise.

In the simulation, we set $\mu = 1$, and total samples $T = 120$ with the sampling interval $\delta = 0.1$ s are involved. The true value of the initial state is $\mathbf{x}_0 = [0, -0.5]^T$ and the estimated initial state is generated by a Gaussian distribution $\mathcal{N}(\mathbf{x}_0, 0.01\mathbf{I}_2)$. The covariance of the process noise and the nominal measurement noise are, respectively, given by $\mathbf{Q}_{t-1} = 0.005\mathbf{I}_2$ and $R_t = 1$. $L = 1000$ Monte Carlo runs are implemented to obtain the simulation results. The time-averaged root mean square (TRMSE) is employed as a metric, which is defined as

$$\text{TRMSE}_k = \frac{1}{T} \sum_{t=1}^T \sqrt{\frac{1}{L} \sum_{i=1}^L (x_{k,t}^i - \hat{x}_{k,t}^i)^2}, \quad k = 1, 2 \quad (26)$$

Fig. 1 illustrates the TRMSEs of x_1 and x_2 with varying φ and fixed $\phi = 0.2$ while Fig. 2 shows these when $\varphi = 200$ and ϕ varies. It can be seen that, as expected, the conventional CKF degrades significantly since the quadratic

loss in the CKF is sensitive to outliers. Overall, among all robust solutions, our proposed DG-MCL-CKF has smallest TRMSEs while the RMCC-CKF has largest ones. The inferior performance of the RMCC-CKF is due primarily to the linearization error during the linear regression procedure. The Huber-CKF performs comparably against to the MCC-CKF, the performance of which is significantly influenced by the kernel parameters. This is illustrated by the fact that the MCC-CKF1 outperforms the MCC-CKF2. Similar conclusions can also be drawn from Fig. 3 in which we present the RMSE of the two components of the state for the different algorithms in the scenario that when $\phi = 0.3$ and $\varphi = 200$.

We have further studied how the parameter α influences the performance of the proposed method. Table 1 presents the TRMSEs of x_1 and x_2 in the two selected scenarios with different α . Obviously, our method degrades to the MCC-CKF1 when $\alpha = 1$ while it turns to be the MCC-CKF2 when $\alpha = 0$. From the results one can observe that the DG-MCL-CKF (i.e., $\alpha \neq 1$ or $\alpha \neq 0$) outperforms both the MCC-CKF1 and MCC-CKF2, so the mixture correntropy is superior over the conventional correntropy. This may bring us a heuristic idea for designing a correntropy related robust Kalman filtering algorithm, i.e., using the mixture correntropy with a larger kernel parameter and a relative small one to alternate the original correntropy to skip the kernel parameter selection step. The optimal value of α , however, still needs further investigation.

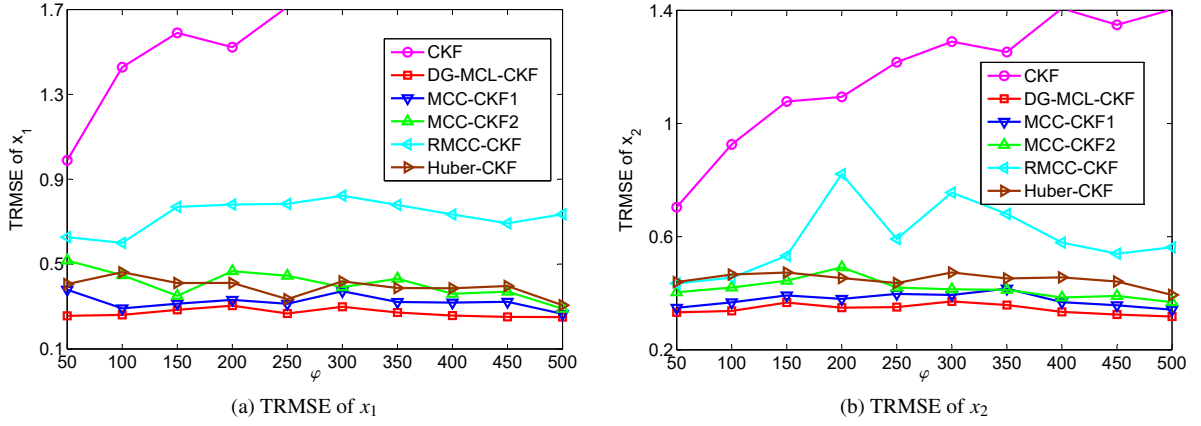


Figure 1: TRMSEs of different algorithms with varying φ with fixed $\phi = 0.2$.

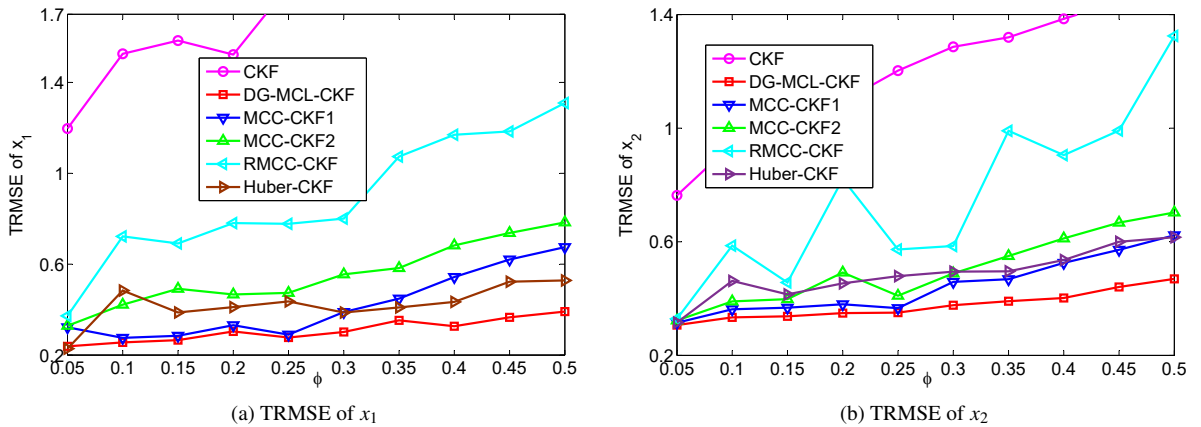


Figure 2: TRMSEs of different algorithms with varying ϕ with fixed $\varphi = 200$.

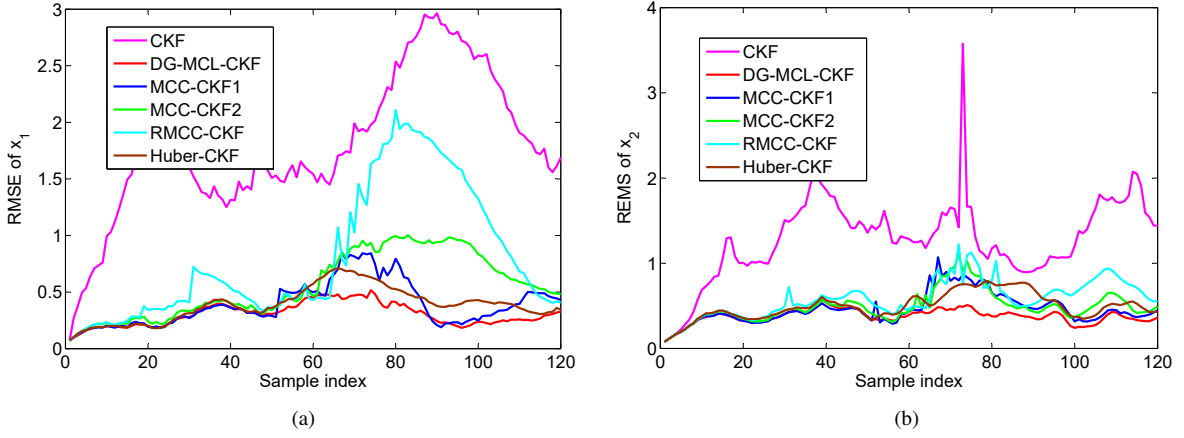


Figure 3: RMSE of x_1 and x_2 when $\phi = 0.3$ and $\varphi = 200$.

Table 1: TRMSE of x_1 and x_2 with different α

α		0(MCC-CKF1)	0.1	0.3	0.5	0.7	0.9	1(MCC-CKF2)
$\phi = 0.3, \varphi = 200$	x_1	0.4245	0.3692	0.3625	0.3631	0.3650	0.3578	0.4912
	x_2	0.4792	0.4243	0.4180	0.4154	0.4154	0.4127	0.5004
$\phi = 0.2, \varphi = 300$	x_1	0.2726	0.2665	0.2599	0.2544	0.2498	0.2458	0.3640
	x_2	0.3522	0.3387	0.3327	0.3280	0.3243	0.3213	0.3709

5. Conclusion

In this paper, we have investigated an outlier-robust CKF based on mixture correntropy for a nonlinear system involving the heavy-tailed measurement noise. The mixture correntropy induced loss is employed to replace the quadratic loss for the measurement fitting error in the conventional Kalman filtering framework. The resulting robust Kalman filtering problem is then iteratively solved by the conventional CKF with a reweighted covariance matrix of the measurement noise. It can be noted for the simulation results that the proposed algorithm can outperform the existing MCC based solutions.

Appendix A. Cubature Kalman Filter [8]

For a state space model described in (7) and (8) with the Gaussian process and measurement noise, the CKF is implemented as follows:

Step 1: Initialize the initial state $\mathbf{x}_0 \sim \mathcal{N}(\hat{\mathbf{x}}_{0|0}, \mathbf{P}_{0|0})$ and generate the basic weighted cubature point set $\{\xi_i, \eta_i\}$ for $i = 1, \dots, 2n$, where n is the dimension of the state, $\xi_i = \sqrt{n}[\mathbf{I}]_i$, $[\mathbf{I}] = [\mathbf{I}_n, -\mathbf{I}_n]$ and $\eta_i = 1/(2n)$.

Step 2: Generate the sigma points related to distribution $\mathcal{N}(\hat{\mathbf{x}}_{t-1|t-1}, \mathbf{P}_{t-1|t-1})$ as

$$\mathbf{P}_{t-1|t-1} = \mathbf{S}_{t-1|t-1} \mathbf{S}_{t-1|t-1}^T \quad (\text{A.1})$$

$$\xi_{i,t-1} = \mathbf{S}_{t-1|t-1} \xi_i + \hat{\mathbf{x}}_{t-1|t-1} \quad (\text{A.2})$$

Step 3: Calculate the predicted state and its associated error covariance

$$\chi_{i,t-1} = f(\xi_{i,t-1}) \quad (\text{A.3})$$

$$\hat{\mathbf{x}}_{t|t-1} = \sum_{i=1}^{2n} \eta_i \chi_{i,t-1} \quad (\text{A.4})$$

$$\mathbf{P}_{t|t-1} = \sum_{i=1}^{2n} \eta_i (\chi_{i,t-1} - \hat{\mathbf{x}}_{t|t-1})(\chi_{i,t-1} - \hat{\mathbf{x}}_{t|t-1})^T + \mathbf{Q}_{t-1} \quad (\text{A.5})$$

Step 4: Generate the sigma points for the predicted distribution $\mathcal{N}(\hat{\mathbf{x}}_{t|t-1}, \mathbf{P}_{t|t-1})$

$$\mathbf{P}_{t|t-1} = \mathbf{S}_{t|t-1} \mathbf{S}_{t|t-1}^T \quad (\text{A.6})$$

$$\phi_{i,t} = \mathbf{S}_{t|t-1} \xi_i + \hat{\mathbf{x}}_{t|t-1} \quad (\text{A.7})$$

Step 5: Calculate the predicted measurement, predicted measurement covariance and state-measurement covariance

$$\psi_{i,t} = h(\phi_{i,t}), \hat{\mathbf{y}}_t = \sum_{i=1}^{2n} \eta_i \psi_{i,t} \quad (\text{A.8})$$

$$\mathbf{P}_{yy} = \sum_{i=1}^{2n} \eta_i (\psi_{i,t} - \hat{\mathbf{y}}_t)(\psi_{i,t} - \hat{\mathbf{y}}_t)^T + \mathbf{R}_t \quad (\text{A.9})$$

$$\mathbf{P}_{xy} = \sum_{i=1}^{2n} \eta_i (\chi_{i,t} - \hat{\mathbf{x}}_{t|t-1})(\psi_{i,t} - \hat{\mathbf{y}}_t)^T \quad (\text{A.10})$$

Step 6: Obtain the filtered state and its associated error covariance

$$\hat{\mathbf{x}}_{t|t} = \hat{\mathbf{x}}_{t|t-1} + \mathbf{K}_t(\mathbf{y}_t - \hat{\mathbf{y}}_t) \quad (\text{A.11})$$

$$\mathbf{P}_{t|t} = \mathbf{P}_{t|t-1} - \mathbf{K}_t \mathbf{P}_{yy} \mathbf{K}_t^T \quad (\text{A.12})$$

$$\mathbf{K}_t = \mathbf{P}_{xy} \mathbf{P}_{yy}^{-1} \quad (\text{A.13})$$

References

- [1] M. S. Grewal, A. P. Andrews, Applications of Kalman filtering in aerospace 1960 to the present [historical perspectives], IEEE Control Systems Magazine 30 (3) (2010) 69–78.
- [2] F. Auger, M. Hilaret, J. M. Guerrero, E. Monmasson, T. Orlowska-Kowalska, S. Katsura, Industrial applications of the Kalman filter: A review, IEEE Transactions on Industrial Electronics 60 (12) (2013) 5458–5471.
- [3] P. Lu, L. Van Eykeren, E. Van Kampen, C. De Visser, Q. Chu, Adaptive three-step Kalman filter for air data sensor fault detection and diagnosis, Journal of Guidance, Control, and Dynamics (null) (2015) 590–604.
- [4] H. Wang, H. Yu, M. Hoy, J. Dauwels, H. Wang, Variational Bayesian dynamic compressive sensing, in: 2016 IEEE International Symposium on Information Theory (ISIT), IEEE, 2016, pp. 1421–1425.
- [5] T.-S. Lou, L. Wang, H. Su, M.-W. Nie, N. Yang, Y. Wang, Desensitized cubature Kalman filter with uncertain parameters, Journal of the Franklin Institute 354 (18) (2017) 8358–8373.
- [6] R. E. Kalman, A new approach to linear filtering and prediction problems, Journal of basic Engineering 82 (1) (1960) 35–45.
- [7] S. J. Julier, J. K. Uhlmann, Unscented filtering and nonlinear estimation, Proceedings of the IEEE 92 (3) (2004) 401–422.
- [8] I. Arasaratnam, S. Haykin, Cubature Kalman filters, IEEE Transactions on Automatic Control 54 (6) (2009) 1254–1269.
- [9] H. Wang, W. Zhang, J. Zuo, H. Wang, Generalized cubature quadrature Kalman filters: derivations and extensions, Journal of Systems Engineering and Electronics 28 (3) (2017) 556–562.
- [10] M. S. Arulampalam, S. Maskell, N. Gordon, T. Clapp, A tutorial on particle filters for online nonlinear/non-Gaussian Bayesian tracking, IEEE Transactions on signal processing 50 (2) (2002) 174–188.
- [11] C. D. Karlgaard, H. Schaub, Huber-based divided difference filtering, Journal of guidance, control, and dynamics 30 (3) (2007) 885–891.
- [12] C. D. Karlgaard, Nonlinear regression Huber–Kalman filtering and fixed-interval smoothing, Journal of guidance, control, and dynamics 38 (2) (2014) 322–330.
- [13] L. Chang, K. Li, Unified form for the robust Gaussian information filtering based on M-estimate, IEEE Signal Processing Letters 24 (4) (2017) 412–416.

- [14] H. Wang, H. Li, W. Zhang, H. Wang, Laplace ℓ_1 robust Kalman filter based on majorization minimization, in: 2017 20th International Conference on Information Fusion (Fusion), IEEE, 2017, pp. 1–5.
- [15] X. Luan, F. Liu, P. Shi, h_∞ filtering for nonlinear systems via neural networks, *Journal of the Franklin Institute* 347 (6) (2010) 1035–1046.
- [16] W. Liu, P. P. Pokharel, J. C. Principe, Correntropy: Properties and applications in non-Gaussian signal processing, *IEEE Transactions on Signal Processing* 55 (11) (2007) 5286–5298.
- [17] W. Ma, H. Qu, G. Gui, L. Xu, J. Zhao, B. Chen, Maximum correntropy criterion based sparse adaptive filtering algorithms for robust channel estimation under non-Gaussian environments, *Journal of the Franklin Institute* 352 (7) (2015) 2708–2727.
- [18] X. Luo, Y. Xu, W. Wang, M. Yuan, X. Ban, Y. Zhu, W. Zhao, Towards enhancing stacked extreme learning machine with sparse autoencoder by correntropy, *Journal of The Franklin Institute* 355 (4) (2018) 1945–1966.
- [19] G. T. Cinar, J. C. Principe, Hidden state estimation using the correntropy filter with fixed point update and adaptive kernel size, in: The 2012 International Joint Conference on Neural Networks (IJCNN), IEEE, 2012, pp. 1–6.
- [20] R. Izanloo, S. A. Fakoorian, H. S. Yazdi, D. Simon, Kalman filtering based on the maximum correntropy criterion in the presence of non-Gaussian noise, in: 2016 Annual Conference on Information Science and Systems (CISS), IEEE, 2016, pp. 500–505.
- [21] B. Chen, X. Liu, H. Zhao, J. C. Principe, Maximum correntropy Kalman filter, *Automatica* 76 (2017) 70–77.
- [22] G. Wang, N. Li, Y. Zhang, Maximum correntropy unscented Kalman and information filters for non-Gaussian measurement noise, *Journal of the Franklin Institute* 354 (18) (2017) 8659–8677.
- [23] M. V. Kulikova, Square-root algorithms for maximum correntropy estimation of linear discrete-time systems in presence of non-Gaussian noise, *Systems & Control Letters* 108 (2017) 8–15.
- [24] H. Wang, H. Li, W. Zhang, J. Zuo, H. Wang, Maximum correntropy derivative-free robust Kalman filter and smoother, *IEEE Access* 6 (2018) 70794–70807.
- [25] Y. Wang, L. Yang, Q. Ren, A robust classification framework with mixture correntropy, *Information Sciences* 491 (2019) 306–318.